



Identical patterns of cortico-efferent tract involvement in primary lateral sclerosis and amyotrophic lateral sclerosis: A tract of interest-based MRI study

Hans-Peter Müller, Martin Gorges, Rebecca Kassubek, Johannes Dorst, Albert C. Ludolph, Jan Kassubek*

Department of Neurology, University of Ulm, Germany

ARTICLE INFO

Keywords:

Diffusion tensor imaging
Amyotrophic lateral sclerosis
Primary lateral sclerosis
Magnetic resonance imaging
Motor neuron diseases

ABSTRACT

Background: There is an ongoing debate whether primary lateral sclerosis (PLS) should be regarded as an independent disease entity separate from amyotrophic lateral sclerosis (ALS) or as a slowly progressive variant of ALS.

Objective: The study was designed to investigate specific white matter alterations in diffusion tensor imaging (DTI) data from PLS patients by a hypothesis-guided tract-of-interest-based approach compared with ‘classical’ ALS patients and healthy controls, in order to identify microstructural changes according to the neuropathologically defined ALS affection pattern in vivo.

Methods: DTI-based white matter mapping was performed both by an unbiased voxelwise statistical comparison and by a hypothesis-guided tractwise analysis of fractional anisotropy (FA) maps according to the ALS-staging pattern for 50 PLS and 50 ALS patients vs 50 matched controls.

Results: The analysis of white matter integrity by regional FA reductions demonstrated the characteristic alteration patterns along the CST and also in frontal and prefrontal brain areas in PLS patients and ALS patients. In the tract-specific analysis according to the ALS-staging pattern, PLS and ALS affection patterns showed identical significant alterations of ALS-related tract systems when compared with controls and no differences when compared with each other.

Conclusions: This DTI study showed the same microstructural affection patterns in PLS patients as in ALS, in support of the hypothesis that PLS is a phenotypical variant of ALS.

1. Introduction

Primary lateral sclerosis (PLS) is considered a motor neuron disease (MND) which almost exclusively affects upper motor neurons (UMN) (Wais). Since the first descriptions by Jean-Martin Charcot in 1874 (calling it “primary sclerosis of the lateral columns”) and Wilhelm Erb in 1902, the debate is still ongoing whether PLS should be regarded as an independent disease entity separate from amyotrophic lateral sclerosis (ALS) or as a slowly progressive variant of ALS (Singer et al., 2007). In the revision of the El Escorial criteria, it is held for PLS (as one of the restricted phenotypes) that it develops into ALS in the vast majority of patients (Ludolph et al., 2015). A specific classification of MND patients is a challenge of growing importance in the light of the continuous efforts of clinical trials with the option that the therapeutic portfolio for ALS might expand, also reflected in the initiative to revise the diagnostic criteria (Ludolph et al., 2015). The diagnostic proof as

definite ALS in a given patient with a PLS phenotype might be provided *ex vivo* by the neuropathological demonstration of cerebral TDP43 pathology according to the neuropathological staging concept of ALS by Braak et al. (2013), Brettschneider et al. (2013), and Braak et al. (2017). In order to assess this neuropathological pattern in MND patients in vivo by magnetic resonance imaging, the hypothesis-guided tract-of-interest-based diffusion tensor imaging technique of the brain has been established (Kassubek et al., 2014; Müller et al., 2016; Kassubek et al., 2018). By this approach, it was possible to demonstrate for another restricted ALS phenotype, i.e. lower motor neuron disease with fast disease progression, an affection pattern for corticoefferent fibers as defined for ALS, that way supporting that fast progressing LMND is a phenotypical variant of ALS (Rosenbohm et al., 2016; Müller et al., 2018). In analogy, we studied a group of PLS patients' brain MRI for disease-associated patterns of microstructural WM alterations corresponding to those detectable in ALS, to test the hypothesis that PLS

* Corresponding author at: Dept. of Neurology, University of Ulm, Oberer Eselsberg 45, 89081 Ulm, Germany.
E-mail address: jan.kassubek@uni-ulm.de (J. Kassubek).

<https://doi.org/10.1016/j.nicl.2018.03.018>

Received 28 December 2017; Received in revised form 28 February 2018; Accepted 14 March 2018

Available online 15 March 2018

2213-1582/ © 2018 The Authors. Published by Elsevier Inc. This is an open access article under the CC BY-NC-ND license (<http://creativecommons.org/licenses/by-nc-nd/4.0/>).

shows the same pattern like ALS, in this case supporting the assumption that PLS is a variant of ALS with a specific clinical phenotype.

2. Methods

2.1. Subjects and patient characteristics

Fifty PLS patients were included who met the proposed diagnostic criteria for PLS (Pringle et al., 1992; Singer et al., 2007; Wais et al., 2017). To be eligible, subjects had to meet the following criteria: no family history of MND, no clinical diagnosis of frontotemporal dementia (FTD), age at onset > 40 years, no mutations of major genes related to hereditary spastic paraparesis if investigated, no other major systemic, psychiatric or neurological illnesses, no history of substance abuse. Further mandatory criteria for inclusion were negative tests for multiple sclerosis and for central nervous system infections, and routine MRI scans excluded any brain or cervical cord abnormalities suggesting a different etiology of the clinical symptoms. Disease duration in the PLS group was 5 ± 3 years (range 3 to 21 years), and age of onset of the motor disorder was 58 ± 11 years (all data are given as arithmetic mean \pm standard deviation (SD)). All patients underwent standardized clinical, neurological, and routine laboratory examinations. A composite UMN burden score was derived from evaluating the number of pathologic reflexes elicited from 15 body sites as previously described (Turner et al., 2004) (Table 1). Cognitive status was estimated from the Edinburgh Cognitive and Behavioural ALS Screen (ECAS – Lulé et al., 2015) and was available for 22 out of 50 PLS patients.

PLS patients presented a revised ALS functional rating scale (ALS-FRS-R) (Cedarbaum et al., 1999) of 36 in average (minimum 16, maximum 45). All subjects gave written informed consent for the study protocol according to institutional guidelines which had been approved by the Ethics Committee of Ulm University, Germany (No. 19/12).

A group of 50 ALS patients were selected to match for age and gender to the PLS group. The diagnosis of all cases was made according to the El Escorial diagnostic criteria (Ludolph et al., 2015), all these patients showed clinical involvement of the first and the second motor neuron and showed no clinical diagnosis of frontotemporal dementia (FTD), ALS patients presented with an ALS-FRS-R of 35 in average (minimum 16, maximum 46); thus no differences in ALS-FRS-R between the PLS group and the ALS group were found. ECAS and was available for 13 out of 50 ALS patients (Table 1).

None of the patients with ALS or PLS had any history of other neurological or psychiatric disorders. PLS and ALS patients were compared to age- and gender-matched controls. Gross brain pathology including vascular brain alterations was excluded by conventional MRI. All healthy control subjects had no family history of neuromuscular

disease and had no history of neurologic, psychiatric, or other major medical illnesses and were recruited from among spouses of patients and by word of mouth.

A summary of the subjects' characteristics is given in Table 1. The group comparison concerning age by Kruskal-Wallis test showed 0.30, concerning gender by Kruskal-Wallis test revealed 0.38, thus indicating no significant differences for the different subject groups.

2.2. MRI acquisition

DTI scanning was performed on a 1.5 Tesla Magnetom Symphony (Siemens Medical, Erlangen, Germany); two DTI study protocols were used, 61 subjects (19 PLS patients, 21 ALS patients, and 21 controls) were scanned with protocol A, and 89 subjects (31 PLS patients, 29 ALS patients, and 29 controls) were scanned with protocol B. DTI study protocol A consisted of 13 volumes (45 slices, 128×128 pixels, slice thickness 2.2 mm, pixel size $1.5 \text{ mm} \times 1.5 \text{ mm}$) representing 12 gradient directions ($b = 800 \text{ s/mm}^2$) and one scan with gradient 0 ($b = 0$). The echo time (TE) and repetition time (TR) were 93 ms and 8000 ms, respectively. Five scans were averaged online by the scanner software in image space. DTI study protocol B consisted of 52 volumes (64 slices, 128×128 pixels, slice thickness 2.8 mm, pixel size $2.0 \text{ mm} \times 2.0 \text{ mm}$), representing 48 gradient directions ($b = 1000 \text{ s/mm}^2$) and four scans with $b = 0$. TE and TR were 95 ms and 8000 ms.

2.3. Data analysis

The postprocessing and statistical analysis was performed by use of the analysis software *Tensor Imaging and Fiber Tracking* (TIFT – Müller et al., 2007a). In order to spatially normalize the data to the Montreal Neurological Institute (MNI) stereotaxic space, study-specific templates were created and MNI normalization was performed iteratively (Müller and Kassubek, 2013). From the stereotaxically normalized DTI data sets, DTI metrics' maps (fractional anisotropy – FA, mean diffusivity – MD, axial diffusivity – AD, radial diffusivity - RD) maps were calculated for quantitative mapping of microstructure (Le Bihan et al., 2001). FA is a summary measure of microstructural integrity. While FA is highly sensitive to microstructural changes, it is less specific to the type of change. MD is an inverse measure of the membrane density, AD tends to be variable in WM changes and axonal injury, and RD increases in WM with dysmyelination. Changes in the axonal diameters or density may also influence RD (Song et al., 2002). In a consecutive step, an 8 mm (FWHM) Gaussian filter was applied for smoothing of DTI metrics' maps in order to achieve a good balance between sensitivity and specificity (Unrath et al., 2010).

DTI metrics' maps of controls recorded with the different protocols

Table 1
Subjects' characteristics.

	PLS	ALS	Controls	p
Male/female	29/21	22/28	25/25	Kruskal-Wallis: 0.375
Age/years (mean \pm std. dev.)	62 ± 10 Range (42–86)	58 ± 10 Range (20–79)	58 ± 16 Range (19–78)	Kruskal-Wallis: 0.304
ALS-FRS-R (mean \pm std. dev.)	36 ± 8 Range (16–45)	35 ± 8 Range (16–46)	–	t-Test: 0.9
ALS-FRS-r slope (48-ALS-FRS-R)/(disease duration/years)	3 ± 3 Range (0–10)	10 ± 9 Range (0–40)	–	t-Test: 0.00002
Disease duration/years (mean \pm std. dev.)	5 ± 3 Range (3–21)	2 ± 2 Range (0–8)	–	t-Test: 0.0002
ECAS	99 ± 24 Range (64–124) ^a	106 ± 14 Range (71–123) ^b	–	t-Test: 0.30
UMN burden score	9 ± 5 Range (4–16)	7 ± 4 Range (1–15)	–	t-Test: 0.063

ALS-FRS-R – revised ALS functional rating scale. ECAS – Edinburgh Cognitive and Behavioural ALS Screen, UMN burden score – Upper Motor Neuron Burden Score.

^a ECAS was available for 22 out of 50 PLS patients.

^b ECAS was available for 13 out of 50 ALS patients.

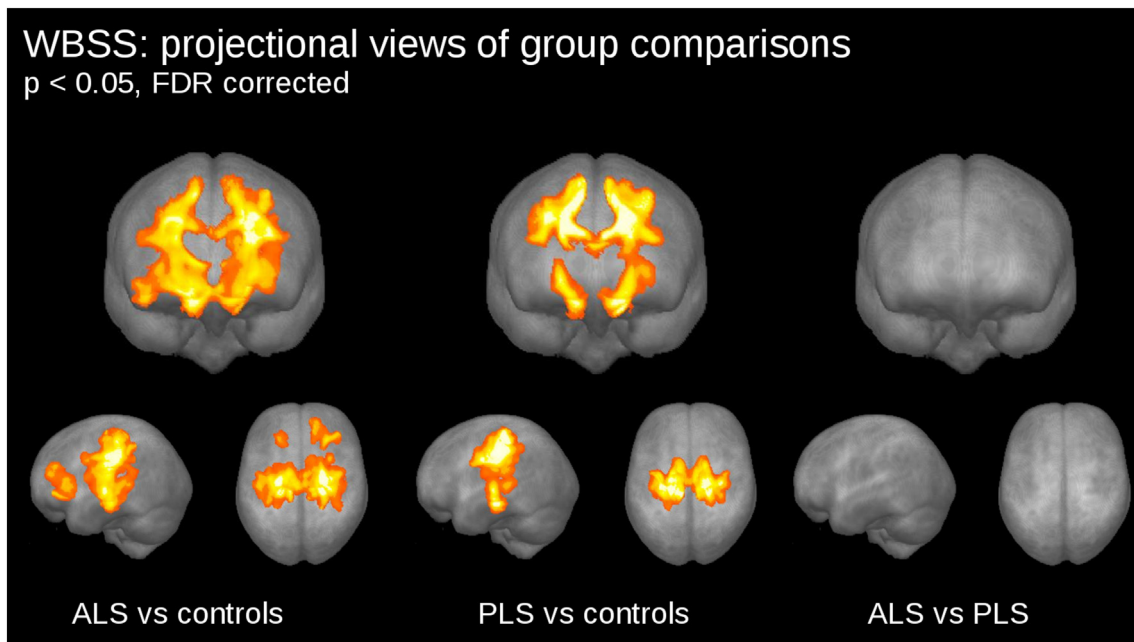


Fig. 1. Whole brain-based spatial statistics (WBSS) of FA maps at the group level for ALS patients, PLS patients, and controls. WBSS of FA maps demonstrated multiple clusters of regional FA reductions at $p < 0.05$ (corrected for multiple comparisons, FDR), projectional views.

were used for calculation of 3D-correction matrices according to a previously reported protocol (Müller et al., 2016; Roskopf et al., 2015). Then, DTI metrics' maps of PLS and ALS patients and controls were harmonized by application of the respective 3-D correction matrix (linear first order correction). In the final step, DTI metrics' maps of all subjects were corrected for the covariate age.

Statistical comparison by Student's t -test was performed voxelwise for FA values to detect changes between the subject groups – WBSS. Voxels with FA values below 0.2 were not considered for calculation as cortical grey matter shows FA values up to 0.2 (Kunimatsu et al., 2004).

Statistical results were corrected for multiple comparisons using the false-discovery-rate (FDR) algorithm at $p < 0.05$ (Genovese et al., 2002). Further reduction of the alpha error was performed by a spatial correlation algorithm that eliminated isolated voxels or small isolated groups of voxels in the size range of the smoothing kernel leading to a threshold cluster size of 256 voxels.

Pathways for defined brain structures according to the ALS-staging system (Braak et al., 2013; Brettschneider et al., 2013) were identified with a seed-to-target approach as previously described (Kassubek et al., 2014; Kassubek et al., 2018; Rosenbohm et al., 2016). TOIs for the definition of the four ALS stages were used as previously defined, i.e. the corticospinal tract (CST, representative for stage 1), the corticorubral and corticopontine tracts (representative for stage 2), the corticostriatal pathway (representative for stage 3), and the proximal perforant path (representative for stage 4) (Kassubek et al., 2014; Kassubek et al., 2018). As a reference path, the tract was used originating from the corpus callosum (CC) area V where no involvement in ALS-associated neurodegeneration could be anticipated. Tractwise fractional anisotropy statistics (TFAS – Müller et al., 2007b) was performed by statistically comparing the FA values in a respective tract system between two subject groups (Student's t -test). Accordingly, maps of the other DTI metrics were used to perform the equivalent analysis, respectively.

For statistical comparison at the group level, WBSS and TFAS analysis used Student's t -test as the subject groups were large enough to show a Gaussian distribution of FA values. However, Mann-Whitney- U test shows almost identical statistical results.

2.4. Data analysis after normalization for disease duration

PLS patients, as expected, exhibited considerably higher disease duration than ALS cases, with values ranging from 3 to 21 years. Moreover, PLS cases showed a slower progression rate than the ALS group. Both disease duration and progression rate can exert a significant impact on FA values. In a previous study in lower motor neuron disease (Müller et al., 2018), a postprocessing approach was used to normalize FA values for disease duration. Even if the original criteria (Pringle et al., 1992) proposed a minimum of 3 years of disease duration for the diagnosis of PLS, recent guidelines defined cases with 4 years of disease duration as suspected PLS-dominant ALS and these are considered as uncertain classification (Singer et al., 2007; Gordon et al., 2006).

Thus, as an additional analysis, FA values were normalized to the identical timepoint of disease duration of 4 years. In a defined voxel or tract structure, the average FA decrease per year

$$\langle \Delta FA \rangle_{ALS, year} = \Delta FA_{(controls-ALS)} / \langle DD \rangle_{ALS} \quad (1)$$

for ALS patients was defined by the difference in FA between controls and ALS patients divided by the average disease duration of ALS patients.

The average progression rate in ALS patients was calculated by arithmetically averaging the individual progression rates

$$\langle R \rangle_{ALS} = \langle (48 - ALS - FRS - R) / DD \rangle_{ALS-patients} \quad (2)$$

The individual FA loss per year was then estimated by $\Delta FA_{ALS, year}$ weighted by the ratio of individual progression rate and the average progression rate in ALS patients and PLS patients as follows.

$$\begin{aligned} \Delta FA_{year, ALS} &= \langle \Delta FA \rangle_{ALS, year} * R / \langle R \rangle_{ALS} \\ \Delta FA_{year, PLS} &= \langle \Delta FA \rangle_{ALS, year} * R / \langle R \rangle_{PLS} \end{aligned} \quad (3)$$

The individual FA value for the defined timepoint 4 years can then be calculated by

$$FA_{4years} = FA_{scan} + (DD - 4years) \Delta FA_{year, ALS/PLS} \quad (4)$$

This normalization for disease duration was performed for averaged FA values of tract structures (TFAS) as well as a voxelwise analysis prior to WBSS.

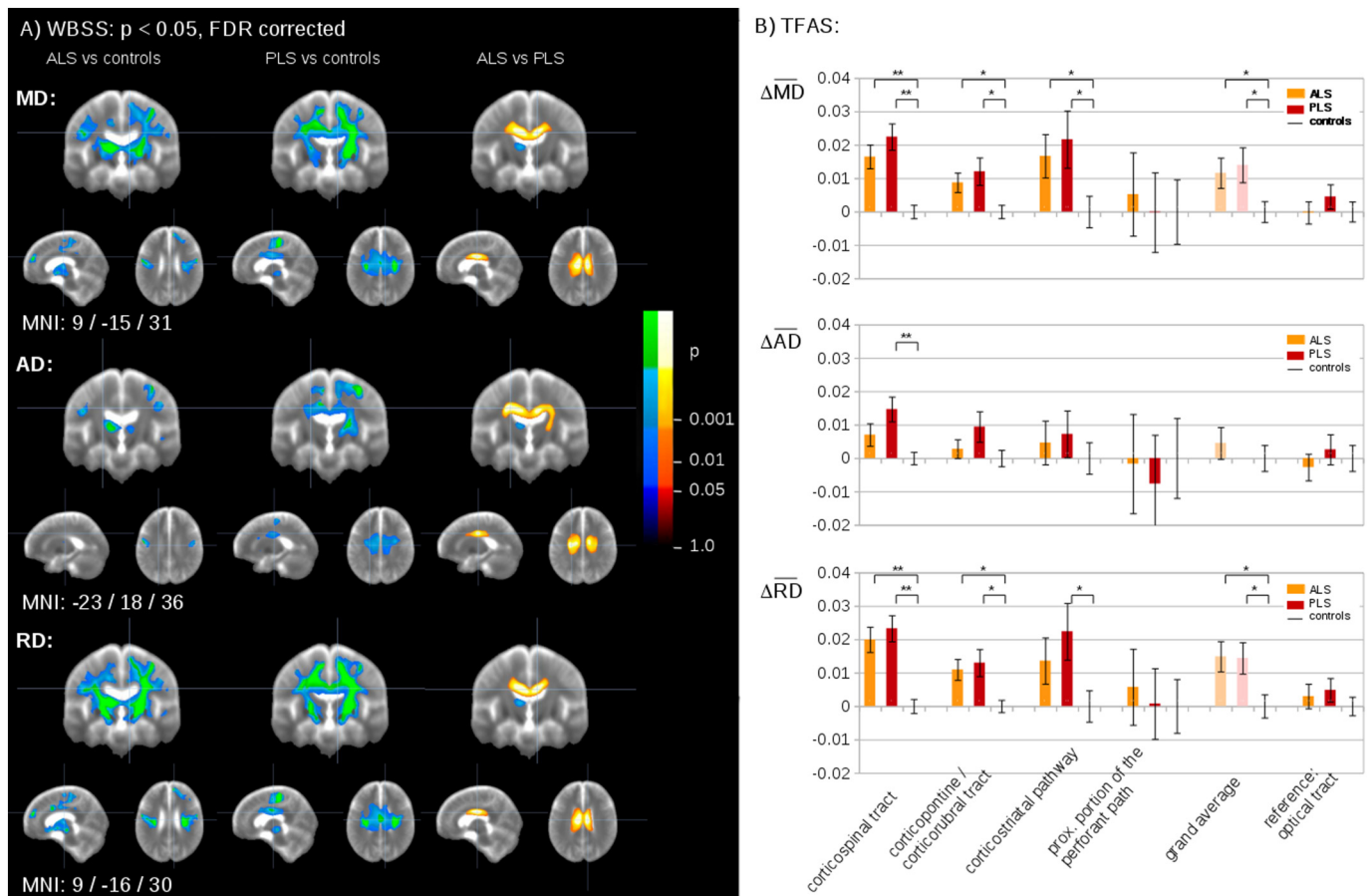


Fig. 2. (A) Whole brain-based spatial statistics (WBSS) of mean diffusivity (MD), axonal diffusivity (AD), and radial diffusivity (RD) maps at the group level for ALS patients, PLS patients, and controls at $p < 0.05$ (corrected for multiple comparisons, FDR). Compared with controls, both the PLS group and the ALS group showed increases of AD, RD, and MD primarily along the CST with smaller clusters bihemispherically in the frontal and also in the temporal lobes. The PLS group showed regional increases in MD, AD, and RD in the corpus callosum (CC) area 3. (B) Tractwise fractional anisotropy statistics (TFAS) of MD, AD, and RD maps at the group level for ALS patients, PLS patients, and controls. TFAS demonstrated significant regional differences of DTI-metrics between ALS patients and controls as well as between PLS patients and controls in ALS-related tract systems and in the grand average. MD, AD, RD values were given as differences of ALS/PLS patients vs controls (ΔMD , ΔAD , ΔRD). No alterations between groups were observed in the reference tract. * $p < 0.05$, ** $p < 0.001$.

3. Results

3.1. Whole brain-based spatial statistics of FA maps

The comparison at the group level by WBSS for PLS patients, ALS patients, and controls demonstrated multiple clusters of regional alterations at $p < 0.05$ (corrected for multiple comparisons, FDR). Projectional views for the maps of FA reductions are depicted in Fig. 1 for the group comparisons. Comparing the ALS patients to the controls, widespread FA reduction along the CST and also in frontal and prefrontal brain areas was observed. PLS patients also showed a widespread FA reduction pattern compared to controls (similar to ALS patients vs controls), while ALS patients vs PLS patients showed no significant FA alterations. The WBSS analysis of FA maps provided almost identical results for ALS and PLS groups, but the comparison between ALS patients and healthy controls showed a small cluster of reduced FA in prefrontal WM (Fig. 1), whereas this cluster did not show up in the PLS vs healthy controls comparison.

Fig. 2 shows the analysis for the other DTI metrics MD, AD, and RD. Compared with controls, both the PLS group and the ALS group show increases of AD, RD, and MD primarily along the CST with smaller clusters bihemispherically in the frontal and also in the temporal lobes. The PLS group showed regional increases in MD, AD, and RD in the corpus callosum (CC) area 3 (Hofer and Frahm, 2006), indicating both axonal injury and dysmyelination especially in PLS compared to ALS and controls. In Table 2, a summary of WBSS clusters for all DTI metrics

(FA, AD, RD, MD) is provided.

Trends could be found in the PLS group for the correlation analyses of disease duration and ALS-FRS-R, respectively, with all DTI metrics of tract systems (stage 1 to 4-related tract systems); however, none of the correlations was significant.

3.2. Differences of FA in the tract systems

The hypothesis-guided analysis of the FA differences in the ALS-related tract systems by use of TFAS showed differences of the averaged FA values between the ALS and the control groups as well as between the PLS and the control groups; both, ALS and PLS group vs the control group showed most prominent FA alterations in the CST, followed by FA reductions in the other ALS-staging-related tracts (Fig. 3). For unified scales for all tract systems, FA, MD, AD, RD values were given as differences between ALS/PLS patients and controls (ΔFA , ΔMD , ΔAD , ΔRD) in Figs. 2 and 3. Here, significant FA reductions could be observed independently for the CST, for the corticopontine and the corticorubral tract, for the corticostriatal pathway, and for the proximal portion of the perforant path (ALS stages 1–4) in PLS patients and ALS patients each compared to controls. For the grand average of the stage-related tract systems, significant FA reductions were observed for PLS patients and ALS patients compared to controls. No significant FA alterations were found for any group comparison in the reference path. The small cluster of reduced FA in prefrontal WM in the comparison between ALS patients and healthy controls in the WBSS analysis was mirrored by the

Table 2
Clusters from whole brain-based spatial statistics.

Cluster no.	Cluster size	MNI x/y/z (maximum)		p		Anatomical localization
<i>Fractional anisotropy (FA)</i>						
ALS vs controls						
F1	75,150	23/–23/37	L/R	< 0.000001	Decrease	CST
F2	2280	15/36/–4	R	< 0.000001	Decrease	Frontal lobe
F3	636	–22/26/–1	L	< 0.000001	Decrease	Frontal lobe
PLS vs controls						
F4	53,669	23/–26/38	L/R	< 0.000001	Decrease	CST
<i>Axial diffusivity (AD)</i>						
ALS vs controls						
A1	6303	–12/–8/12	L/R	< 0.000001	Increase	Striatum
A2	3033	38/–17/60	R	< 0.000001	Increase	CST
A3	2514	–52/–14/34	L	< 0.000001	Increase	Temporal lobe
A4	1972	50/3/15	R	< 0.000001	Increase	Temporal lobe
A5	1839	56/–8/31	R	< 0.000001	Increase	Temporal lobe
A6	1137	18/–37/54	R	< 0.000001	Increase	CST
A7	850	49/–24/–1	R	< 0.000001	Increase	Temporal lobe
PLS vs controls						
A8	44,998	36/–17/54	L/R	< 0.000001	Increase	CST
A9	1228	–33/10/5		< 0.000001	Increase	Frontal lobe
ALS vs PLS						
A10	25,305	–23/–18/36	L/R	< 0.000001	Decrease	CC area 3
<i>Radial diffusivity (RD)</i>						
ALS vs controls						
R1	100,650	–29/–24/37	L/R	< 0.000001	Increase	CST
R2	15,984	43/37/–3	R	< 0.000001	Increase	Frontal lobe
R3	6093	–30/20/–9	L	< 0.000001	Increase	Frontal lobe
R4	1682	33/9/42	R	< 0.000001	Increase	Temporal lobe
R5	1588	–43/5/20	L	< 0.000001	Increase	Temporal lobe
R6	1563	–11/28/24	L	< 0.000001	Increase	Frontal lobe
PLS vs controls						
R7	101,549	–23/–22/39	L/R	< 0.000001	Increase	CST
ALS vs PLS						
R8	20,709	9/–16/30	L/R	< 0.000001	Decrease	CC area 3
<i>Mean diffusivity (MD)</i>						
ALS vs controls						
M1	58,081	30/–19/36	L/R	< 0.000001	Increase	CST
M2	13,189	–57/–7/32	L	< 0.000001	Increase	Temporal lobe
M3	11,901	43/37/–3	R	< 0.000001	Increase	Frontal lobe
M4	4764	30/19/–9	L	< 0.000001	Increase	Frontal lobe
M5	1642	–49/8/23	L	< 0.000001	Increase	Temporal lobe
M6	1413	33/9/42	R	< 0.000001	Increase	Temporal lobe
PLS vs controls						
M7	96,194	24/–21/38	L/R	< 0.000001	Increase	CST
ALS vs PLS						
M8	23,815	9/–15/31	L/R	< 0.000001	Decrease	CC area 3

WBSS (p < 0.05, FDR-corrected) of FA, AD, RD, MD maps.

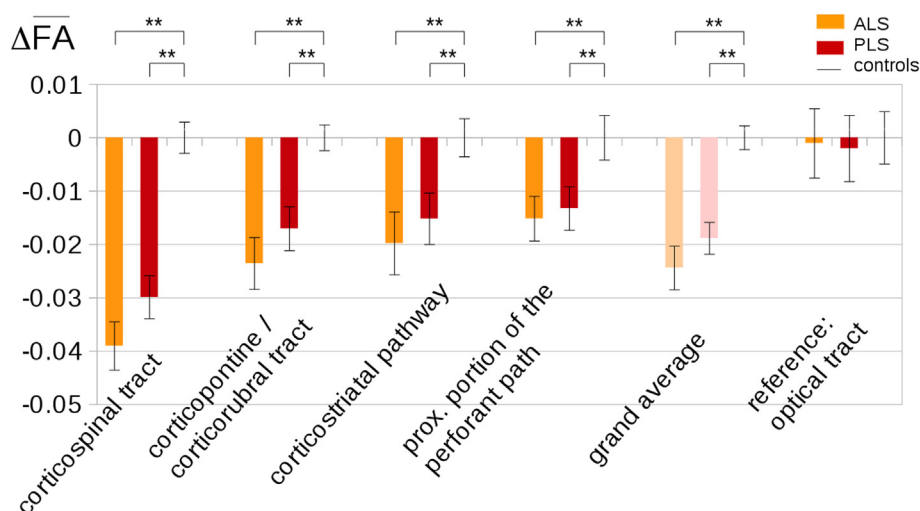


Fig. 3. Tractwise fractional anisotropy statistics (TFAS) of FA maps at the group level for ALS patients, PLS patients, and controls. TFAS demonstrated significant regional FA reductions in ALS-related tract systems and in the grand average between ALS patients and controls as well as between PLS patients and controls. FA values were provided as differences of ALS/PLS patients vs controls (Δ FA). No alterations between groups were observed in the reference tract. ******p < 0.001.

Table 3

p-Values for differences between groups for different ALS-related tract systems. Significant DTI metrics' alterations ($p < 0.05$) are coloured.

	CST (stage 1)	Corticopontine/ corticorubral tract (stage 2)	Corticostriatal pathway (stage 3)	Proximal portion of the perforant path (stage 4)	Grand average	Reference
FA						
ALS vs controls	$2 * 10^{-10}$	$4 * 10^{-5}$	$5 * 10^{-3}$	0.01	$1 * 10^{-6}$	0.9
PLS vs controls	$4 * 10^{-8}$	$6 * 10^{-4}$	0.01	0.03	$2 * 10^{-6}$	0.8
ALS vs PLS	0.1	0.3	0.5	0.7	0.3	0.9
MD						
ALS vs controls	$1 * 10^{-4}$	0.01	0.04	0.7	0.04	0.9
PLS vs controls	$2 * 10^{-6}$	0.01	0.03	0.9	0.02	0.3
ALS vs PLS	0.2	0.5	0.6	0.7	0.7	0.3
AD						
ALS vs controls	0.07	0.5	0.6	0.9	0.5	0.6
PLS vs controls	$9 * 10^{-4}$	0.07	0.4	0.8	0.7	0.7
ALS vs PLS	0.1	0.2	0.8	0.7	0.3	0.4
RD						
ALS vs controls	$2 * 10^{-5}$	$3 * 10^{-3}$	0.1	0.7	0.01	0.5
PLS vs controls	$1 * 10^{-6}$	$5 * 10^{-3}$	0.02	0.9	0.02	0.3
ALS vs PLS	0.2	0.6	0.6	0.4	0.5	0.7

differences in the corticopontine/corticorubral tract systems and also in the corticostriatal pathway in the TFAS analysis. For PLS, the regional prefrontal WM alteration in WBSS was below the level of significance at cluster level, but there were significant FA alterations in the corresponding tract systems, i.e. the corticopontine/corticorubral tract and the corticostriatal pathway.

A summary of all alterations in the tract systems at the group level is provided in Table 3. Fig. 2 shows the respective analysis for the other DTI metrics MD, AD, and RD.

3.3. Differences of FA after normalization for disease duration

Projectional views for the maps of FA reductions are depicted in Supplementary Fig. 1A for the group comparisons after normalization for disease duration. Comparing the ALS patients with the controls, widespread FA reductions along the CST and also in frontal and prefrontal brain areas were observed; PLS patients also showed FA reductions along the CST compared to controls, while ALS patients vs PLS patients showed widespread FA reduction along the CST and also in frontal and prefrontal brain areas. Compared to the WBSS without normalization for disease duration (Fig. 1), the results of the comparison PLS patients vs controls were almost identical (given that average disease duration was 4 years anyway), whereas the effect of

normalization for disease duration further emphasized the alterations of the ALS group (given that an average disease duration of 2 years was normalized to 4 years) (Fig. 1). A similar effect could be observed for the TFAS results (Supplementary Fig. 1B): alterations of ALS patients after normalization for disease duration were emphasized leading to significant differences between all subject groups for all tract systems. Thus, it could be concluded that FA alterations were increased in ALS patients compared to PLS patients with respect to disease duration and progression rate.

4. Discussion

PLS is strictly defined as a syndrome in which the disease begins with upper motor neuron deficits existing in isolation, while ALS according to the El Escorial criteria as published in the year 2000 (Brooks et al., 2000), requires both evidence of lower motor neuron degeneration by clinical, electrophysiological or neuropathologic examination and evidence of UMN degeneration by clinical examination. It is a long-standing discussion that the well-established phenotype PLS is one which awaits a better definition (by clinical or technical approaches) in order both to improve the inclusion into clinical trials for ALS patients where appropriate and to support access to health care systems (Agosta et al., 2015; Ludolph et al., 2015). In the current study, the application

of the DTI-based in vivo transfer of the neuropathologically-defined cerebral propagation scheme according to the proposed Braak staging for ALS (Braak et al., 2013; Kassubek et al., 2014) could be applied to PLS patients, with results as could be obtained in ALS patients with the ‘classical’ clinical presentation of involvement of the first and the second motor neuron (Kassubek et al., 2018). The hypothesis that PLS shows the same pattern like ALS could thus be verified, i.e. both unbiased WBSS as well as hypothesis-guided tract of interest-based TFAS demonstrated affection patterns like in ALS. The clinical differences between ALS and PLS might be explained by a higher vulnerability of the second motoneuron in ALS patients which cannot be addressed by brain DTI.

On the basis of these neuroimaging data, the proposed staging scheme for ALS (Braak et al., 2013) can be considered valid also for PLS. TOI-based DTI supports the clinical view of PLS as an ALS variant and is in strong favour of the consequence to treat these patients like ALS, including the opportunity to be enrolled in clinical trials. These findings are an analogy of the demonstration of corticofugal tract involvement in fast progressive lower motor neuron disease by the same approach (Rosenbohm et al., 2016) which had been confirmed in a two-centre study with an additional sample of 28 LMND patients in whom a central nervous system involvement had not been shown by a data-driven DTI analysis (Müller et al., 2018). In a further analogy, previous data-driven neuroimaging studies in PLS using DTI or other imaging techniques could not specifically demonstrate the involvement of the corticoefferent tracts – beyond CST – which had been defined according to the ALS-associated pTDP-43 pathology pattern in the brain (Agosta et al., 2014). The classification of PLS as an ALS subtype rather than an independent disease entity, as supposed by the current neuroimaging study, is further supported by similar spreading patterns and multi system degeneration characteristics (Wais et al., 2017), genetic overlaps (Brugman et al., 2005; van Rheenen et al., 2012), common biomarkers like neurofilaments (Steinacker et al., 2018), and TDP-43 pathology patterns (Kosaka et al., 2012). However, this hypothesis still has to be further confirmed by more extensive neuropathological research analyzing pTDP-43 and its spreading pattern and new biomarkers (Wais et al., 2017).

This study was not without limitations. First, the neuropathological confirmation of the DTI-based in vivo transfer of the ALS propagation in the brain by autopsy results is lacking for the patients who have been classified by MRI. Second, the design of the current study was cross-sectional, while only longitudinal data from different timepoints during the course of the disease would allow to address the sequential spreading model and the relationship between the tract alterations and the clinical development at the individual patient level – specifically, since the different disease course in PLS makes further analyses of this phenotype desirable (Kassubek et al., 2018). Finally, this study was performed with different study protocols, but scanning-protocol-based differences in FA maps could be corrected for by technical ex post facto harmonization (Roskopf et al., 2015) as previously used in multicentre studies (Müller et al., 2016). This constellation paths the way to multicentre studies making use of the TOI-based technique also in multicentre data in PLS patients from different sites, as previously done in LMND (Müller et al., 2018). A further limitation of this study was that the DTI data were collected over a comparatively long period; thus, no unified cognitive score could be reported for the complete subject sample.

In summary, the results of this study confirm the clinical approach to the phenotype of PLS as an ALS variant, in accordance with the latest revision of the El Escorial criteria for ALS (Ludolph et al., 2015; Agosta et al., 2015). Taken together, the TOI-based DTI studies in PLS and LMND are in further support of a clinicopathologic continuum of MND spanning PLS, ALS, and LMND. It might be a straightforward conclusion from these data that the expectation that “neuroimaging approaches might help to arrange PLS in the MND spectrum and its classification” (Wais et al., 2017) could be fulfilled. As such, this study might be

considered a further milestone in the process of establishing MRI as a biological marker in ALS and its variants (Filippi et al., 2015).

Supplementary data to this article can be found online at <https://doi.org/10.1016/j.nicl.2018.03.018>.

Author contributions

Hans-Peter Müller: study concept and design, data analysis and interpretation of data, critical revision of manuscript for intellectual content

Johannes Dorst: Data collection, interpretation of data, critical revision of manuscript for intellectual content

Martin Gorges: Data collection, data analysis, critical revision of manuscript for intellectual content

Albert Ludolph: Interpretation of data, study supervision, critical revision of manuscript for intellectual content

Jan Kassubek: study concept and design, interpretation of data, study supervision, drafting of manuscript.

Author disclosures

All authors: none for this study.

Acknowledgements

Sonja Fuchs is thankfully acknowledged for her great help in the acquisition of MRI data. The authors would like to thank the Ulm University Center for Translational Imaging MoMAN for its support.

Funding

This study was supported by the German Research Foundation (Deutsche Forschungsgemeinschaft, DFG Grant Number LU 336/15-1) and the German Network for Motor Neuron Diseases (BMBF 01GM1103A).

Statement

All human studies have been approved by the appropriate ethics committee and have therefore been performed in accordance with the ethical standards laid down in the 1964 Declaration of Helsinki and its later amendments.

References

- Agosta, F., Galantucci, S., Riva, N., et al., 2014. Intrahemispheric and interhemispheric structural network abnormalities in PLS and ALS. *Hum. Brain Mapp.* 35, 1710–1722.
- Agosta, F., Al-Chalabi, A., Filippi, M., et al., 2015. The El Escorial criteria: strengths and weaknesses. *Amyotroph. Lateral Scler. Frontotemporal Degener.* 16, 1–7.
- Braak, H., Brettschneider, J., Ludolph, A.C., et al., 2013. Amyotrophic lateral sclerosis - a model of corticofugal axonal spread. *Nat. Rev. Neurol.* 9, 708–714.
- Braak, H., Neumann, M., Ludolph, A.C., et al., 2017. Does sporadic amyotrophic lateral sclerosis spread via axonal connectivities? *Neurol. Int. Open* 1, E136–E141.
- Brettschneider, J., Del Tredici, K., Toledo, J.B., et al., 2013. Stages of pTDP-43 pathology in amyotrophic lateral sclerosis. *Ann. Neurol.* 74, 20–38.
- Brooks, B.R., Miller, R.G., Swash, M., et al., 2000. El Escorial revisited: revised criteria for the diagnosis of amyotrophic lateral sclerosis. *Amyotroph. Lateral Scler. Other Motor Neuron Disord.* 1, 293–299.
- Brugman, F., Wokke, J.H., Vianney de Jong, J.M., et al., 2005. Primary lateral sclerosis as a phenotypic manifestation of familial ALS. *Neurology* 64, 1778–1779.
- Cedarbaum, J.M., Stambler, N., Malta, E., et al., 1999. The ALSFRS-R: a revised ALS functional rating scale that incorporates assessments of respiratory function. *BDNF ALS Study Group (Phase III).* *J. Neurol. Sci.* 169, 13–21.
- Filippi, M., Agosta, F., Grosskreutz, J., et al., 2015. Progress towards a neuroimaging biomarker for amyotrophic lateral sclerosis. *Lancet Neurol.* 14, 786–788.
- Genovese, C.R., Lazar, N.A., Nichols, T., 2002. Thresholding of statistical maps in functional neuroimaging using the false discovery rate. *NeuroImage* 15, 870–878.
- Gordon, P.H., Cheng, B., Katz, I.B., et al., 2006. The natural history of primary lateral sclerosis. *Neurology* 66, 647–653.
- Hofer, S., Frahm, J., 2006. Topography of the human corpus callosum revisited - comprehensive fiber tractography using diffusion tensor magnetic resonance imaging. *NeuroImage* 32, 989–994.

- Kassubek, J., Müller, H.P., Del Tredici, K., et al., 2014. Diffusion tensor imaging analysis of sequential spreading of disease in amyotrophic lateral sclerosis confirms patterns of TDP-43 pathology. *Brain* 137, 1733–1740.
- Kassubek, J., Müller, H.P., Del Tredici, K., et al., 2018. Imaging the pathoanatomy of amyotrophic lateral sclerosis in vivo: targeting a propagation-based biological marker. *J. Neurol. Neurosurg. Psychiatry* 89, 374–381 (pii: jnnp-2017-316365).
- Kosaka, T., Fu, Y.J., Shiga, A., et al., 2012. Primary lateral sclerosis: upper-motor-predominant amyotrophic lateral sclerosis with frontotemporal lobar degeneration—immunohistochemical and biochemical analyses of TDP-43. *Neuropathology* 32, 373–384.
- Kunimatsu, A., Aoki, S., Masutani, Y., et al., 2004. The optimal trackability threshold of fractional anisotropy for diffusion tensor tractography of the corticospinal tract. *Magn. Reson. Med. Sci.* 3, 11–17.
- Le Bihan, D., Mangin, J.F., Poupon, C., et al., 2001. Diffusion tensor imaging: concepts and applications. *J. Magn. Reson. Imaging* 13, 534–546.
- Ludolph, A., Drory, V., Hardiman, O., et al., 2015. A revision of the El Escorial criteria - 2015. *Amyotroph. Lateral Scler. Frontotemporal Degener.* 29, 1–2.
- Lulé, D., Burkhardt, C., Abdulla, S., et al., 2015. The Edinburgh Cognitive and Behavioural Amyotrophic Lateral Sclerosis Screen: a cross-sectional comparison of established screening tools in a German-Swiss population. *Amyotroph. Lateral Scler. Frontotemporal Degener.* 16, 16–23.
- Müller, H.P., Kassubek, J., 2013. Diffusion tensor magnetic resonance imaging in the analysis of neurodegenerative diseases. *J. Vis. Exp.*(77).
- Müller, H.P., Unrath, A., Ludolph, A.C., et al., 2007a. Preservation of diffusion tensor properties during spatial normalization by use of tensor imaging and fibre tracking on a normal brain database. *Phys. Med. Biol.* 52, N99–109.
- Müller, H.P., Unrath, A., Sperfeld, A.D., et al., 2007b. Diffusion tensor imaging and tractwise fractional anisotropy statistics: quantitative analysis in white matter pathology. *Biomed. Eng. Online* 6, 42.
- Müller, H.P., Turner, M.R., Grosskreutz, J., et al., 2016. A large-scale multicentre cerebral diffusion tensor imaging study in amyotrophic lateral sclerosis. *J. Neurol. Neurosurg. Psychiatry* 87, 570–579.
- Müller, H.P., Agosta, F., Riva, N., et al., 2018. Fast progressive lower motor neuron disease is an ALS variant: a two-centre tract of interest-based MRI data analysis. *Neuroimage Clin.* 17, 145–152.
- Pringle, C.E., Hudson, A.J., Munoz, D.G., et al., 1992. Primary lateral sclerosis. Clinical features, neuropathology and diagnostic criteria. *Brain* 115, 495–520.
- Rosenbohm, A., Müller, H.P., Hübers, A., et al., 2016. Corticoefferent pathways in pure lower motor neuron disease: a diffusion tensor imaging study. *J. Neurol.* 263, 2430–2437.
- Roskopf, J., Müller, H.P., Dreyhaupt, J., et al., 2015. Ex post facto assessment of diffusion tensor imaging metrics from different MRI protocols: preparing for multicentre studies in ALS. *Amyotroph. Lateral Scler. Frontotemporal Degener.* 16, 92–101.
- Singer, M.A., Statland, J.M., Wolfe, G.I., Barohn, R.J., 2007. Primary lateral sclerosis. *Muscle Nerve* 35, 291–302.
- Song, S.-K., Sun, S.-W., Ramsbottom, M.J., et al., 2002. Demyelination revealed through MRI as increased radial (but unchanged axial) diffusion of water. *NeuroImage* 17, 1429–1436.
- Steinacker, P., Verde, F., Fang, L., et al., 2018. Chitotriosidase (CHIT1) is increased in microglia and macrophages in spinal cord of amyotrophic lateral sclerosis and cerebrospinal fluid levels correlate with disease severity and progression. *J. Neurol. Neurosurg. Psychiatry* 89, 239–247.
- Turner, M.R., Cagnin, A., Turkheimer, F.E., et al., 2004. Evidence of widespread cerebral microglial activation in amyotrophic lateral sclerosis: an [11C](R)-PK11195 positron emission tomography study. *Neurobiol. Dis.* 15, 601–609.
- Unrath, A., Müller, H.P., Riecker, A., et al., 2010. Whole brain-based analysis of regional white matter tract alterations in rare motor neuron diseases by diffusion tensor imaging. *Hum. Brain Mapp.* 31, 1727–1740.
- van Rheenen, W., van Blitterswijk, M., Huisman, M.H., et al., 2012. Hexanucleotide repeat expansions in C9ORF72 in the spectrum of motor neuron diseases. *Neurology* 79, 878–882.
- Wais, V., Rosenbohm, A., Petri, S., et al., 2017. The concept and diagnostic criteria of primary lateral sclerosis. *Acta Neurol. Scand.* 136, 204–211.